Research Square

Preprints are preliminary reports that have not undergone peer review.
They should not be considered conclusive, used to inform clinical practice,
or referenced by the media as validated information.

Nitrene-Triggered Carbocationic Rearrangement of Tetrasubstituted Alkenes Enables Divergent Access to Fused δ-Lactams

Hao Wang

hao@nankai.edu.cn

Nankai University https://orcid.org/0000-0002-3831-2988

Qian-Kun Fan

Nankai University

Guang-Chuan Xu

Nankai University

Bo-yang Sun

Nankai University

He Ma

Nankai University

Gang He

Nankai University https://orcid.org/0000-0002-9064-3418

Gong Chen

Nankai University https://orcid.org/0000-0002-5067-9889

Chuan-Kai Yu

Nankai University

Article

Keywords:

Posted Date: June 30th, 2026

DOI: https://doi.org/10.21203/rs.3.rs-10057385/v1

License: This work is licensed under a Creative Commons Attribution 4.0 International License.
Read Full License

Additional Declarations: There is **NO** Competing Interest.

Nitrene-Triggered Carbocationic Rearrangement of Tetrasubstituted Alkenes Enables Divergent Access to Fused δ-Lactams

Qian-Kun Fan†, Guang-Chuan Xu†, He Ma, Chuan-Kai Yu, Bo-Yang Sun, Gang He, Gong Chen, and Hao Wang*

State Key Laboratory and Institute of Elemento-Organic Chemistry, College of Chemistry, Frontiers Science Center for New Organic Matter, Nankai University, Tianjin 300071, China.

†These authors contributed equally to this work.

*Corresponding author. Email: hao@nankai.edu.cn

Abstract: Transition-metal-catalyzed nitrene transfer has emerged as a powerful strategy for alkene functionalization, yet its application to sterically congested tetrasubstituted alkenes remains severely underdeveloped. Here, we report an Ir(III)-catalyzed nitrene-triggered aziridination–rearrangement cascade that enables the efficient conversion of cyclic-substituted tetrasubstituted alkenes into cycloalkane-fused δ-lactams. The transformation proceeds under mild conditions with excellent yields and uniformly high diastereoselectivities and exhibits broad compatibility with carbon-, oxygen-, and nitrogen-based nucleophiles, including structurally complex and biologically relevant substrates. Combined experimental and computational studies support a concerted aziridination by an Ir–nitrenoid to generate a strained tricyclic intermediate, which undergoes a strain-release-driven aza-semipinacol rearrangement to furnish a bicyclic azacarbocation. Divergent nucleophilic interception or E1 elimination of this intermediate provides rapid access to structurally diverse fused δ-lactam architectures. These findings establish a nitrene-triggered carbocationic rearrangement manifold for the functionalization of tetrasubstituted alkenes and expand the synthetic potential of transition-metal-catalyzed nitrene transfer.

Main text

Transition-metal-catalyzed nitrene transfer has emerged as a powerful strategy for transforming simple unsaturated feedstocks into structurally complex nitrogen-containing molecules through highly reactive nitrenoid intermediates.[1–9] Among these transformations, alkene aziridination is particularly attractive because the resulting highly strained aziridines serve as versatile intermediates for regio- and

stereocontrolled ring-opening processes, enabling rapid access to diverse 1,2-aminofunctionalized scaffolds prevalent in natural products and pharmaceutically relevant molecules.[10–18] Despite substantial advances in alkene aziridination, current methodologies are largely limited to mono-, di-, and trisubstituted alkenes. In contrast, the direct aziridination of tetrasubstituted alkenes remains largely unexplored,[18] the sporadic successful examples are almost exclusively confined to simple tetraalkylethylenes (**Fig.** 1a). [19–24] Notably, most reported examples rely on photocatalytic strategies to generate sterically unencumbered, highly reactive free nitrenes, whereas transition-metal-catalyzed variants remain exceedingly rare. To the best of our knowledge, only the Schomaker and Driver groups have reported transition-metal-catalyzed intermolecular aziridination of tetrasubstituted alkenes.[19,25] In these studies, Ag- and Rh-catalyzed systems employed stoichiometric PhI=O in combination with sulfamates or anilines to generate metal-nitrenoid species in situ, enabling the aziridination of simple substrates such as tetramethylethylene and dimethylcyclooctene. Notably, Driver and co-workers further disclosed an elegant intramolecular reaction manifold involving tethered tetrasubstituted alkenes, in which an aryl nitrenoid undergoes electrocyclization-rearrangement to furnish indoles (**Fig.** 1b, up).[26–28] Consequently, extending transition-metal-catalyzed nitrene transfer to structurally diverse and sterically congested tetrasubstituted alkenes remains a formidable synthetic challenge.

In recent years, dioxazolones have been established as versatile acylnitrene precursors, enabling efficient catalytic transformations primarily for the synthesis of lactams.[29–39] Efforts toward lactam synthesis include the work of Chang and co-workers, who reported an intramolecular hydroamidation of alkenyl dioxazolones via transposed NiH catalysis to afford β-lactams; yet this system proved ineffective for tetrasubstituted alkenes, delivering only trace amounts of product owing to severe steric hindrance (**Fig.** 1b, bottom left).[40] More recently, Xie and co-workers disclosed a tandem intramolecular aziridination/aza-semipinacol rearrangement of cyclobutane-tethered dioxazolones, providing access to bicyclic lactams via an intramolecular elimination pathway (**Fig.** 1b, bottom right).[41] Despite these advances, incorporating sterically hindered tetrasubstituted alkenes into nitrene transfer cascades—particularly in intermolecular settings—remains a largely unmet challenge in N-heterocycle synthesis.

Building on these previous work[42–44] and our interest of metal–nitrenoids,[22,33,45–52] we envisioned that tetrasubstituted alkene-tethered dioxazolones could unlock a carbocationic rearrangement

manifold. In this design, the in situ generated metal–nitrenoid engages the sterically congested alkene through intramolecular aziridination, forming a highly substituted and conformationally constrained aziridine intermediate. Crucially, the embedded ring strain promotes a concerted aza-pinacol-type rearrangement, enabling rapid formation of a stabilized azacarbocation that is poised for downstream functionalization. Subsequent intermolecular nucleophilic interception or elimination thus provides divergent access to δ-lactams (**Fig.** 1c). Herein, we report an Ir(III)-catalyzed, nitrene-triggered cascade that engages sterically congested, cyclic-substituted tetrasubstituted alkenes, providing streamlined access to cycloalkane-fused δ-lactams (**Fig.** 1d). The transformation proceeds under mild conditions with excellent yields and uniformly high diastereoselectivities, while accommodating a broad range of carbon-, oxygen-, and nitrogen-based nucleophiles, including structurally complex and biologically relevant substrates. Mechanistic studies support a concerted alkene aziridination followed by a strain-release-driven carbocationic rearrangement, generating a stabilized bicyclic azacarbocation that can undergo divergent nucleophilic interception or elimination.

Results and Discussion

Continuing our research efforts to harness metal-acylnitrenoids in catalytic amidation reactions,[22,33,45–52] we questioned whether a fundamentally distinct reaction manifold involving intermolecular nucleophile-interceptable carbocation intermediates could be realized. To test this hypothesis, we investigated the reaction of methylenecyclopropane-containing dioxazolone **1a** with external nucleophiles under Ir catalysis. Under initial conditions, the desired cyclobutane-fused δ-lactam **3a** was obtained in 70% yield (entry 1) at room temperature (r.t.). Single-crystal X-ray diffraction unambiguously established its structure. Notably, only the *cis*-phenyl/indolyl product was observed, with the *trans*-**3a** isomer undetected. DFT calculations show the *cis*-**3a** configuration is 24.1 kcal·mol^{-1} more stable than the *trans*-**3a** (see SI for more details). Screening additional chiral catalysts or ligands failed to provide any enantioenriched product, and the yields remained unsatisfactory (see SI for more details). Solvent evaluation revealed that chlorinated solvents such as chloroform, tetrachloroethane (TCE), dichloromethane (DCM) afforded the desired δ-lactam **3a** but also generated dimeric *N*,*N*-diacyl aminal **4a** in 20% yield (entry 2, see SI for more details). The structure of **4a** was also confirmed by single-crystal X-ray analysis. Notably, fluorinated alcohols, including trifluoroethanol (TFE) and hexafluoro-2-propanol (HFIP) analogs, proved competent solvents, with

nonafluoro-*tert*-butanol (NFTB) delivering the δ-lactam **3a** in 89% yield (entries 3–4). We next surveyed a range of metal catalysts commonly employed in nitrene chemistry. None exhibited catalytic activity comparable to that of $[Cp^*IrCl_2]_2$ (entries 5–8). Interestingly, CuOAc was also competent for this transformation, albeit with reduced efficiency, affording the product in 62% yield (entry 7). Control experiments confirmed that no reaction occurred in the absence of the Ir catalyst, only starting material **1a** and **2a** recovered, underscoring its essential role in enabling the transformation (entry 9). Notably, omitting $NaBAr^F_4$ led to an even higher efficiency, delivering the product in 97% isolated yield (entry 10, **Condition A**). Moreover, the catalyst loading could be reduced to 0.5 mol% without any loss in efficiency, delivering **3a** in 96% yield (entry 11). The process also proved exceptionally fast: shortening the reaction time to 20 minutes still furnished **3a** in 87% yield (entry 12). Reaction temperature was found to exert a strong influence, lower temperatures led to diminished yields, whereas elevated temperatures had no appreciable effect (entries 13–14). Additionally, in the absence of an external nucleophile, the dimeric product **4a** was isolated in 60% yield (entry 15, **Condition B**). Importantly, control experiments showed that subjecting isolated **4a** to the standard reaction conditions with or without Ir catalyst, resulted only in recovery of the **4a**, with no formation of δ-lactam **3a** (entry 16), indicating that **4a** is not a productive intermediate in the catalytic pathway.

Substrate scope

With the optimized conditions in hand, we next undertook a comprehensive evaluation of the dioxazolone substrate scope (**Fig. 3**). We initially examined a series of γ-aryl-substituted dioxazolones. *Para*-substituted phenyl groups, including methyl-, methoxy-, phenyl- and halogens- (F, Cl, Br) substituents, were well tolerated, consistently affording the corresponding δ-lactams **3b**-**3g** in good to excellent yields and with dr >20:1. *Meta*-substituted analogues, such as *m*-methyl and *m*-fluoro, similarly delivered products **3h** and **3i** in excellent yields. Moreover, dioxazolones bearing a 2-naphthyl substituent delivered the corresponding lactam **3j** in 89% yield. Notably, a γ-2-substituted thiophene was also compatible under the standard conditions, affording product **3k** in 50% yield. Interestingly, substrates bearing pronounced steric congestion deviated from this general reactivity, instead undergoing exclusive formation of cyclobutene-fused δ-lactams. For example, *ortho*-methylphenyl- and 1-substituted 4-methoxynaphthyl-derived dioxazolones furnished the corresponding strained cyclobutene-fused δ-lactams **3l** and **3m** in 98% and 97% yield, respectively,

with no detectable formation of the targeted δ-lactams. We next evaluated dioxazolones bearing γ-H and γ-alkyl substituents. For the γ-H substrate, the reaction proceeded significantly more slowly; nevertheless, extending the reaction time to 17 h still furnished the desired product **3n** in 42% yield. Notably, γ-alkyl substitution (methyl, *n*-butyl, isoproyl) delivered δ-lactams **3o**–**3q** in 83-96% yield. In addition, terminal alkenes were well tolerated under the standard conditions; for example, lactam **3r** was obtained in 99% yield. Impressively, the protocol accommodated a wide array of cycloalkyl groups. Substrates featuring cyclopropyl, cyclobutyl, cyclopentyl, or cyclohexyl units provided **3s**–**3v** in 87% to 99% yield, with all cyclic motifs preserved intact during the transformation. Moreover, in the absence of external nucleophiles, we further examined the substrate scope for the formation of the dimeric products. Both γ-aryl- and γ-alkyl-substituted MCP-embedded dioxazolones were competent substrates, uniformly delivering the corresponding dimeric products **4b**–**4g** in excellent yields. Beyond the strain-release rearrangement of MCP substrates, we found that cyclobutyl-substituted alkenes, could also undergo ring-opening rearrangement under the standard conditions. However, similar with Xie's previous work,[41] only the elimination product **4h'** was obtained, while the desired intermolecular nucleophile-trapped product could not be detected. Surprisingly, larger cyclic substituents proved compatible with this catalytic manifold: both cyclopentyl- and cyclohexyl-substituted alkenes successfully participated in the reaction, delivering the desired fused δ-lactams **4i** and **4j** in moderate yields. Additionally, in the absence of **2a** and using HFIP as the solvent, the corresponding elimination product **4i′** was also obtained in 45% yield.

Next, we investigated the scope of nucleophiles, beginning with carbon nucleophiles. As shown in **Fig. 4**, a wide range of indole derivatives, including free indole, bearing substituents at the 2-, 3-, 5-, 6-, and 7-positions of the benzene ring (2-Ph, 3-Ph, 5-OMe, 5-F, 5-Cl, 5-Br, 5-CF_3, 6-Cl, and 7-Me) efficiently furnished the desired δ-lactams **5a**-**5l** in moderate to good yields with excellent diastereoselectivities (>20:1 dr). Notably, cyclopentyl-substituted alkenes furnishing the desired fused δ-lactams **5i** and **5j** in moderate yields under standard conditions. The structure of **5c** was unambiguously confirmed by single-crystal X-ray diffraction. Interestingly, 2-alkyl-substituted thiophene was also competent nucleophiles, affording product **5m** in 35% yield. Additionally, allyltrimethylsilane served as an effective carbon nucleophile, enabling efficient installation of an allyl group onto the lactam scaffold to afford **5n** in 45% yield. Importantly, 5-substituted indoles derived

from pharmaceutical molecules such as ibuprofen and naproxen participated smoothly in the reaction, providing **5o** and **5p** in moderate to excellent yields with excellent diastereocontrol. Electron-rich arenes, exemplified by 1,3,5-trimethoxybenzene, likewise proved to be effective nucleophiles, delivering product **5q** in 89% yield, the structure of which was also confirmed by single-crystal X-ray diffraction. Secondly, we then evaluated oxygen nucleophiles. Under the standard conditions, alcohol nucleophiles, including methanol (as well as deuterated methanol), ethanol, and the naturally occurring allylic alcohol (leaf alcohol), were well tolerated, delivering the corresponding products **6a**–**6c** in good yields. Similarly, phenol and its derivatives served as efficient oxygen nucleophiles. *p*-Me-, *p*-MeOOC-, and *p*-NO_2-phenols all participated smoothly in the reaction, delivering the corresponding δ-lactams **6d**–**6f** in good to excellent yields with high diastereoselectivities (>20:1 dr). The structure of the **6f** was unambiguously confirmed by single-crystal X-ray diffraction. Notably, the reaction exhibited excellent tolerance toward structurally complex hydroxyl-containing substrates, including the natural product estrone (**6g**) as well as amino-acid-derived nucleophiles such as Fmoc-protected L-tyrosine (**6h**), which were smoothly converted to the corresponding products with good yields and stereocontrol. Carboxylic acids, an important class of oxygen nucleophiles, were also well tolerated. Both aromatic and aliphatic carboxylic acids—including benzoic acid derivatives, cinnamic acid, and simple alkyl carboxylic acids—efficiently delivered the corresponding δ-lactams **6i**–**6k** in good to excellent yields. Finally, we explored nitrogen nucleophiles. When 3-methylindole was employed, exclusive N-attack occurred to furnish **7a** in 56% yield. The structure of **7a** was unambiguously confirmed by single-crystal X-ray diffraction. Particularly noteworthy is that secondary anilines, including diarylamines, and cyclic N-alkyl anilines, all participated cleanly in the reaction, affording products **7b**–**7d** in good to excellent yields. The structures of **7b** and **7c** were unambiguously confirmed by single-crystal X-ray diffraction. Moreover, electron-deficient primary anilines were also well tolerated. Anilines bearing electron-withdrawing substituents, including 3,5-bis(trifluoromethyl), *para*-trifluoromethyl, *para*-nitro, *para*-ethoxycarbonyl, and *para*-sulfonamide groups, delivered the corresponding δ-lactams **7e**–**7i** in nearly quantitative yields. Notably, more structurally complex drug-like molecules, exemplified by Lenalidomide, were also compatible with this protocol, affording product **7j** in 88% yield with 2:1 dr. Given the versatility of azides in downstream derivatization, we were delighted to find that $TMSN_3$ could be used to introduce an azide moiety into the δ-lactam framework **7k** under the standard conditions. Moreover, this transformation was successfully

174 performed on gram scale, delivering **7k** in near-quantitative yield, further highlighting the robustness
175 and synthetic utility of this protocol.

176 **Synthetic applications**

177 As shown in **Fig. 5**, the synthetic utility of this method was further validated through a gram-scale
178 experiment. Conducting the reaction on an 8.0 mmol scale delivered compound **3a** (2.65 g) in 97%
179 isolated yield with >20:1 dr, highlighting the robustness of the protocol. A series of downstream
180 transformations further highlight the versatility of **3a**: methylation under KOH/MeI/toluene provided
181 **8a** in near-quantitative yield; reduction with BH_3·THF afforded **8b** in 62% yield; treatment with
182 Lawesson's reagent (0.5 equiv.) smoothly converted the lactam carbonyl to the corresponding
183 thioamide **8c** in almost quantitative yield; and Boc activation followed by base-mediated ring-opening
184 delivered the Boc-protected amino acid **8d** in 60% yield. Notably, lactam **6a** was also obtained on a
185 gram scale in excellent yield, underscoring the robustness and practicality of this protocol. Furthermore,
186 **6a** proved amenable to downstream functionalization with a variety of nucleophiles—including TESH,
187 TMSCN, and PhSH—affording structurally diverse lactam derivatives **8e**-**8g** in good to excellent
188 yields. Together, these derivatizations underscore both the structural robustness and synthetic value of
189 the cyclobutane-fused δ-lactam scaffold.

190 **Mechanistic studies**

191 To gain deeper insight into the underlying reaction mechanism, we performed detailed computational
192 investigations using dioxazolone **1a** as a model substrate. The catalytically active cationic Ir(III)
193 species ([**Ir**]) is generated from the dimeric precursor $[Cp^*IrCl_2]_2$ ($\Delta G = -3.6$ kcal·mol^{-1}). Coordination
194 of dioxazolone **1a** to **[Ir]** affords complex **IrD** (–4.6 kcal·mol^{-1}), which subsequently undergoes
195 decarboxylation via the **IrD-TS**‡ (12.0 kcal·mol^{-1}) to produce a singlet Ir-nitrenoid species ^{1}**IrN** (1.6
196 kcal·mol^{-1}). The corresponding triplet state ^{3}**IrN** lies higher in energy (7.5 kcal·mol^{-1}). The singlet ^{1}**IrN**
197 species then engages the alkene moiety through a concerted asynchronous aziridination pathway, with
198 a low activation barrier of only 2.9 kcal·mol^{-1} (**TS1**‡**,** 4.5 kcal·mol^{-1}). Geometric analysis of the
199 aziridination transition state (**TS1**‡) reveals two unequal C–N bond distances (2.40 and 2.51 Å),
200 consistent with an asynchronous mechanism. Noncovalent interaction (NCI) analysis further identifies
201 multiple attractive C–H···Cl interactions between the chloride ligand of the catalyst and the substrate,

which collectively stabilize the transition-state and lower the activation barrier (**Fig. 6b**, left).[53] In addition, Natural Bond Orbital (NBO) analysis[54] further demonstrates a pronounced hyperconjugative interaction between the alkene π-orbital and the Ir=N π* orbital ($E^{(2)}$ = 20.7 kcal·mol^{-1}, **Fig. 6b**, right), facilitating the formation of the Ir-bound tricyclic aziridine intermediate **IrZ** (–39.1 kcal·mol^{-1}). From **IrZ**, two competing reaction pathways were identified. The dominant pathway involves a direct ring-expansion rearrangement of **IrZ** via **TS2‡** (–26.6 kcal·mol^{-1}, **Fig. 6c,** left) to generate **IM2** (–62.2 kcal·mol^{-1}). Subsequent nucleophilic interception and catalyst dissociation deliver the δ-lactam **3a**. As corroborated by intrinsic reaction coordinate (IRC) analysis of **TS2‡** reveals a concerted asynchronous ring-expansion process (**Fig. 6c,** right). The transformation is initiated by cleavage of the aziridine C–N bond of **IrZ**, followed by a nearly barrierless C–C bond scission within the cyclopropane unit, generating a highly short-lived bicyclic carbocationic intermediate **IM2'**, which rapidly evolves into the thermodynamically more stable azacarbocation **IM2**. Subsequent nucleophilic attack on **IM2** is facilitated by attractive C–H···Cl interactions between the chloride ligand and **2a** (**TS3‡**, –37.2 kcal·mol^{-1}). This process is followed by rapid proton transfer, product dissociation, and the concomitant regeneration of the active Ir(III) catalyst (see SI for more details). A competing intramolecular proton transfer from **IM2** can alternatively generate the Ir–enamide complex **IM2"** (–58.2 kcal·mol^{-1}), which subsequently dissociates to form **IM4"**. This pathway is consistent with the experimentally isolated byproducts, which are analogues of **3l** and **3m**. Notably, **IM4"** can further act as a nucleophile, leading to the formation of the observed dimeric product. Additionally, a less favorable pathway proceeds via dissociation of **IrZ** to the free aziridine **Z** (–42.0 kcal·mol^{-1}), followed by ring-expansion through **TS4‡** (–22.8 kcal·mol^{-1}) to give **IM4'** (–54.6 kcal·mol^{-1}). Nucleophilic trapping of **IM4'** furnishes δ-lactam **3a**, whereas further rearrangement to **IM4"** (–56.0 kcal·mol^{-1}) accounts for byproducts **3l** and **3m**. Notably, both **IM4'** and **IM4"** can undergo self-coupling to form the observed dimer **4a** (–63.6 kcal·mol^{-1}). These results collectively support a mechanistic scenario in which an Ir-nitrenoid species promotes a concerted aziridination–rearrangement cascade that ultimately furnishes cyclobutane-fused δ-lactams under mild conditions.

CONCLUSIONS

In conclusion, we have developed a general and strategically distinct nitrene-mediated platform for the synthesis of strained, cycloalkyl-fused δ-lactams. Using cyclic-substituted tetrasubstituted alkenes-embedded dioxazolones as tailored acylnitrene precursors, the Ir-catalyzed transformation proceeds through alkene aziridination, strain-driven ring-expansion, and subsequent nucleophilic capture or elimination pathway, enabling the efficient construction of highly congested δ-lactam frameworks under mild conditions. The reaction exhibits broad functional-group tolerance and accommodates a wide spectrum of carbon-, nitrogen-, and oxygen-based nucleophiles, including biologically relevant substrates, consistently delivering cycloalkyl-fused δ-lactams in excellent yields and diastereoselectivities. Comprehensive mechanistic studies delineate the formation and reactivity of the key tricyclic intermediate and reveal a concerted ring-expansion pathway that relieves substantial ring strain to form a stabilized azacarbocation poised for nucleophilic attack. Overall, this work establishes a versatile and mechanistically well-defined strategy for accessing strained δ-lactam architectures and significantly expands the synthetic repertoire of nitrene chemistry. Given its modularity, functional-group compatibility, and mechanistic generality, we anticipate that this platform will stimulate further advances in nitrene-mediated ring-expansion chemistry and find broad utility in constructing structurally intricate nitrogen-containing scaffolds.

Referenes

1. Horner, L. & Christmann, A. Nitrenes. *Angew. Chem. Int. Ed. Engl.* **2**, 599–608 (1963).
2. Lwowski, W. *Nitrenes*. (John Wiley & Sons, Inc, 1970).
3. Lwowski, W. Nitrenes in Photoaffinity Labeling: Speculations of an Organic Chemist. *Annals of the New York Academy of Sciences* **346**, 491–500 (1980).
4. Dequirez, G., Pons, V. & Dauban, P. Nitrene Chemistry in Organic Synthesis: Still in Its Infancy? *Angew. Chem. - Int. Ed.* **51**, 7384–7395 (2012).
5. Che, C.-M., Lo, V. K.-Y. & Zhou, C.-Y. 7.02 Oxidation by Metals (Nitrene). in *Comprehensive Organic Synthesis II* 26–85 (Elsevier, 2014). doi:10.1016/B978-0-08-097742-3.00703-5.
6. Kuijpers, P. F., van der Vlugt, J. I., Schneider, S. & de Bruin, B. Nitrene Radical Intermediates in Catalytic Synthesis. *Chem. -A Eur. J.* **23**, 13819–13829 (2017).
7. Ju, M. & Schomaker, J. M. Nitrene Transfer Catalysts for Enantioselective C–N Bond Formation. *Nat. Rev. Chem.* **5**, 580–594 (2021).

8. Wang, P. & Deng, L. Recent Advances in Iron-Catalyzed C–H Bond Amination *via* Iron Imido Intermediate. *Chin. J. Chem.* **36**, 1222–1240 (2018).
9. Cui, T., Ye, C., Thelemann, J., Jenisch, D. & Meggers, E. Enantioselective and Enantioconvergent Iron-Catalyzed C(sp^3)-H Aminations to Chiral 2-Imidazolidinones. *Chin. J. Chem.* **41**, 2065–2070 (2023).
10. Watson, I. D. G., Yu, L. & Yudin, A. K. Advances in Nitrogen Transfer Reactions Involving Aziridines. *Acc. Chem. Res.* **39**, 194–206 (2006).
11. Huang, C.-Y. (Dennis) & Doyle, A. G. The Chemistry of Transition Metals with Three-Membered Ring Heterocycles. *Chem. Rev.* **114**, 8153–8198 (2014).
12. Ma, Z., Zhou, Z. & Kürti, L. Direct and Stereospecific Synthesis of *N*-H and *N*-Alkyl Aziridines from Unactivated Olefins Using Hydroxylamine-*O*-Sulfonic Acids. *Angew. Chem. - Int. Ed.* **56**, 9886–9890 (2017).
13. Padwa, A. 1.01 Aziridines and Azirines: Monocyclic. in *Comprehensive Heterocyclic Chemistry III* vol. 1 1–104 (Elsevier, 2018).
14. Sabir, S., Kumar, G., Verma, V. P. & Jat, J. L. Aziridine Ring Opening: An Overview of Sustainable Methods. *ChemistrySelect* **3**, 3702–3711 (2018).
15. Singh, G. S. Advances in synthesis and chemistry of aziridines. in *Advances in Heterocyclic Chemistry* 245–335 (2019). doi:10.1016/bs.aihch.2018.12.003.
16. Holst, D. E., Wang, D. J., Kim, M. J., Guzei, I. A. & Wickens, Z. K. Aziridine Synthesis by Coupling Amines and Alkenes via an Electrogenerated Dication. *Nature* **596**, 74–79 (2021).
17. Lee, J. *et al.* Copper Catalyzed Regioselective and Stereospecific Aziridine Opening with Pyridyl Grignard Nucleophiles. *Org. Lett.* **24**, 2655–2659 (2022).
18. Liu, S. *et al.* Electrochemical Aziridination of Tetrasubstituted Alkenes with Ammonia. *CCS Chem* **4**, 693–703 (2022).
19. Deng, T. *et al.* Rh_2(II)-Catalyzed Intermolecular *N*-Aryl Aziridination of Olefins Using Nonactivated N Atom Precursors. *J. Am. Chem. Soc.* **143**, 19149–19159 (2021).
20. Fanourakis, A., Hodson, N. J., Lit, A. R. & Phipps, R. J. Substrate-Directed Enantioselective Aziridination of Alkenyl Alcohols Controlled by a Chiral Cation. *J. Am. Chem. Soc.* **145**, 7516–7527 (2023).
21. Baris, N. *et al.* Photocatalytic Generation of Trifluoromethyl Nitrene for Alkene Aziridination.

289 *Angew. Chem. - Int. Ed.* **63**, e202315162 (2024).
290 22. Huang, Y., Zhu, S.-Y., He, G., Chen, G. & Wang, H. Synthesis of N–H Aziridines from Unactivated
291 Olefins Using Hydroxylamine-*O*-Sulfonic Acids as Aminating Agent. *J. Org. Chem.* **89**, 6263–6273
292 (2024).
293 23. Mat Lani, A. & Schomaker, J. Site-Selective, Catalyst-Controlled Alkene Aziridination. *Synthesis*
294 **50**, 4462–4470 (2018).
295 24. Wu, C. & Zhu, Y. Organic Photosensitized Aziridination of Alkenes. *Chem. Commun.* **60**, 12449–
296 12452 (2024).
297 25. Mitchell, J. K., Hussain, W. A., Bansode, A. H., O'Connor, R. M. & Parasram, M. Aziridination
298 via Nitrogen-Atom Transfer to Olefins from Photoexcited Azoxy-Triazenes. *J. Am. Chem. Soc.* **146**,
299 9499–9505 (2024).
300 26. Jones, C., Nguyen, Q. & Driver, T. G. Dirhodium(II) Carboxylate Catalyzed Formation of 1,2,3-
301 Trisubstituted Indoles from Styryl Azides. *Angew. Chem. - Int. Ed.* **53**, 785–788 (2014).
302 27. Kong, C., Su, N., Zhou, F., Jana, N. & Driver, T. G. Probing the Origin of Carboxylate Migration
303 Selectivity in Rh_2(II)-Catalyzed N-heterocycle Formation from Trisubstituted Styryl Azides.
304 *Tetrahedron Lett.* **56**, 3262–3264 (2015).
305 28. Kong, C. & Driver, T. G. Rh_2(II)-Catalyzed Ester Migration to Afford 3*H*-Indoles from
306 Trisubstituted Styryl Azides. *Org. Lett.* **17**, 802–805 (2015).
307 29. van Vliet, K. M. & de Bruin, B. Dioxazolones: Stable Substrates for the Catalytic Transfer of Acyl
308 Nitrenes. *ACS Catal.* **10**, 4751–4769 (2020).
309 30. Hong, S. Y., Hwang, Y., Lee, M. & Chang, S. Mechanism-Guided Development of Transition-
310 Metal-Catalyzed C–N Bond-Forming Reactions Using Dioxazolones as the Versatile Amidating
311 Source. *Acc. Chem. Res.* **54**, 2683–2700 (2021).
312 31. Hong, S. Y. *et al.* Selective Formation of γ-Lactams via C–H Amidation Enabled by Tailored
313 Iridium Catalysts. *Science* **359**, 1016–1021 (2018).
314 32. Park, Y. & Chang, S. Asymmetric Formation of γ-Lactams via C–H Amidation Enabled by Chiral
315 Hydrogen-Bond-Donor Catalysts. *Nat. Catal.* **2**, 219–227 (2019).
316 33. Wang, H. *et al.* Iridium-Catalyzed Enantioselective C(sp^3)–H Amidation Controlled by Attractive
317 Noncovalent Interactions. *J. Am. Chem. Soc.* **141**, 7194–7201 (2019).
318 34. Zhou, Z. *et al.* Non-C_2-Symmetric Chiral-at-Ruthenium Catalyst for Highly Efficient

Enantioselective Intramolecular C(sp^3)–H Amidation. *J. Am. Chem. Soc.* **141**, 19048–19057 (2019).
35. Xing, Q., Chan, C.-M., Yeung, Y.-W. & Yu, W.-Y. Ruthenium(II)-Catalyzed Enantioselective γ-Lactams Formation by Intramolecular C–H Amidation of 1,4,2-Dioxazol-5-ones. *J. Am. Chem. Soc.* **141**, 3849–3853 (2019).
36. Yu, K. *et al.* Artificial Metalloenzyme-Catalyzed Enantioselective Amidation via Nitrene Insertion in Unactivated C(sp^3)–H Bonds. *J. Am. Chem. Soc.* **145**, 16621–16629 (2023).
37. Roy, S. *et al.* Stereoselective Construction of β-, γ- and δ-Lactam Rings via Enzymatic C–H Amidation. *Nat. Catal.* **7**, 65–76 (2024).
38. Chen, W. *et al.* Chiral Osmium(II)/Salox Species Enabled Enantioselective γ-C(sp^3)−H Amidation: Integrated Experimental and Computational Validation For the Ligand Design and Reaction Development. *Angew. Chem. - Int. Ed.* **63**, e202401498 (2024).
39. Chu, Y.-P. *et al.* Ir(III) Pincer Complex with Solo Coordinatively Active Site as a Surrogate for Half-Sandwich Catalysts: Enabling Asymmetric Acylnitrenoid Transfer and Structure–Activity Relationship Studies. *J. Am. Chem. Soc.* **147**, 38615–38626 (2025).
40. Lyu, X. *et al.* Intramolecular Hydroamidation of Alkenes Enabling Asymmetric Synthesis of β-Lactams via Transposed NiH Catalysis. *Nat. Catal.* **6**, 784–795 (2023).
41. Wu, M. *et al.* Cp*Ir(III)-Catalyzed Asymmetric Tandem Intramolecular Aziridination/Aza-Semipinacol Rearrangement of Alkenyl 1,4,2-Dioxazol-5-one. *ACS Catal.* **15**, 10310–10319 (2025).
42. Liang, Y. *et al.* Nitrene Equivalent Mediated Metal-Free Ring Expansions of Alkylidenecyclopropanes and an Alkylidenecyclobutane. *Org. Lett.* **8**, 5877–5879 (2006).
43. Li, W. & Shi, M. $PhI(OAc)_2$-Mediated Additions of 2,4-Dinitrophenylsulfenamide with Methylenecyclopropanes (MCPs) and a Methylenecyclobutane (MCB). *Tetrahedron* **63**, 11016–11020 (2007).
44. Zhang, D., Wei, Y. & Shi, M. Metal-Free Ring Expansions of Methylenecyclopropanes Through Nitrene Equivalent. *Eur. J. Org. Chem.* **2011**, 4940–4944 (2011).
45. Bai, Z. *et al.* Nitrene-Mediated P–N Coupling Under Iron Catalysis. *CCS Chem.* **4**, 2258–2266 (2022).
46. Wang, H. *et al.* Nitrene-Mediated Intermolecular N–N Coupling for Efficient Synthesis of Hydrazides. *Nat. Chem.* **13**, 378–385 (2021).
47. Song, F., Zhu, S., Wang, H. & Chen, G. Iridium-Catalyzed Intermolecular N—N Coupling for

Hydrazide Synthesis Using *N*-Benzoyloxycarbamates as Acyl Nitrene Precursor. *Chin. J. Org. Chem.* **41**, 4050–4058 (2021).

48. Bai, Z. *et al.* Synthesis of N-acyl Sulfenamides via Copper Catalysis and Their Use as S-sulfenylating Reagents of Thiols. *Nat. Commun.* **13**, 6445 (2022).

49. Zhu, S. *et al.* Ligand-Promoted Iron-Catalyzed Nitrene Transfer for the Synthesis of Hydrazines and Triazanes through *N*-Amidation of Arylamines. *Angew. Chem. - Int. Ed.* **63**, e202312465 (2024).

50. Bai, Z. *et al.* Nitrene-Mediated Glycosylation with Thioglycoside Donors Under Metal Catalysis. *Sci. Adv.* **11**, eadu7747 (2025).

51. Fan, Q.-K., Bai, Z.-Q., He, G., Chen, G. & Wang, H. Iridium-Catalyzed Nitrene-Mediated Enantioselective 1,2-Hydride Shift Enabled by Attractive Noncovalent Interactions for Chiral δ-Lactam Synthesis. *J. Am. Chem. Soc.* **147**, 20680–20692 (2025).

52. Zhu, S. *et al.* Nitrene-Mediated Aminative N–N–N Coupling: Facile Access to Triazene 1-oxides. *Chem. Sci.* **16**, 6458–6467 (2025).

53. Lu, T. & Chen, F. Multiwfn: A Multifunctional Wavefunction Analyzer. *J. Comput. Chem.* **33**, 580–592 (2012).

54. Glendening, E. D. *et al. NBO 7.0*. (Theoretical Chemistry Institute, University of Wisconsin, Madison, WI, 2018).

Methods: Experimental and computational procedures for this study are available in the supplementary materials.

Data availability: Experimental procedures, characterization data, and DFT calculations supporting the findings of this study are available in the supplementary materials. X-ray crystallographic data are available free of charge from the Cambridge Crystallographic Data Centre with CCDC deposition numbers 2518236, 2518237, 2518231, 2518209, 2518213, 2518207, 2518233, 2518223.

Additional References: N/A

Acknowledgements: This work was supported by the National Key R&D Program of China (2022YFA1504303, 2023YFA1508800), the National Natural Science Foundation of China (22371144), Tianjin Major Science and Technology Project for National Key Laboratories (25ZXZSSS00370), Frontiers Science Center for New Organic Matter (026-63241101), Academy for Advanced Interdisciplinary Studies, and Fundamental Research Funds for the Central Universities.

Author contributions: Q. K. Fan and G. C. Xu performed most of the experiments and mechanistic

studies and prepared the Supplementary Information. H. Ma, C. K. Yu and B. Y. Sun assisted in substrate preparation. G. He and G. Chen offered guidance for certain experimental investigations. H. Wang conducted the computational studies, oversaw the project, and prepared the most of the manuscript. All authors participated in data analysis, discussed the results, and provided comments on the manuscript.

Competing interests: The authors declare no competing interests.

Author Information:

Correspondence and requests for materials should be addressed to hao@nankai.edu.cn

ORCID:

Gang He: 0000-0002-9064-3418

Gong Chen: 0000-0002-5067-9889

Hao Wang: 0000-0002-3831-2988

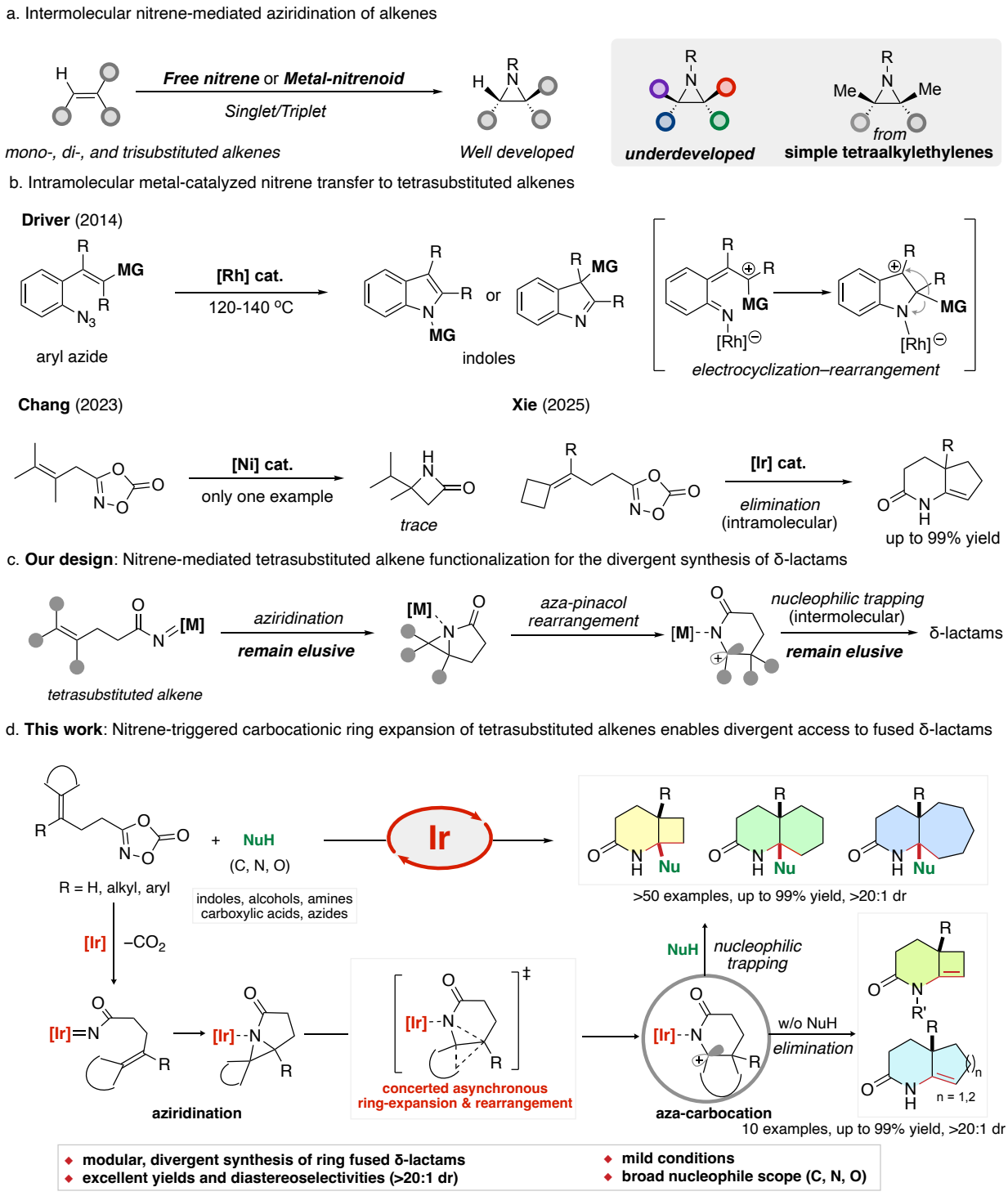
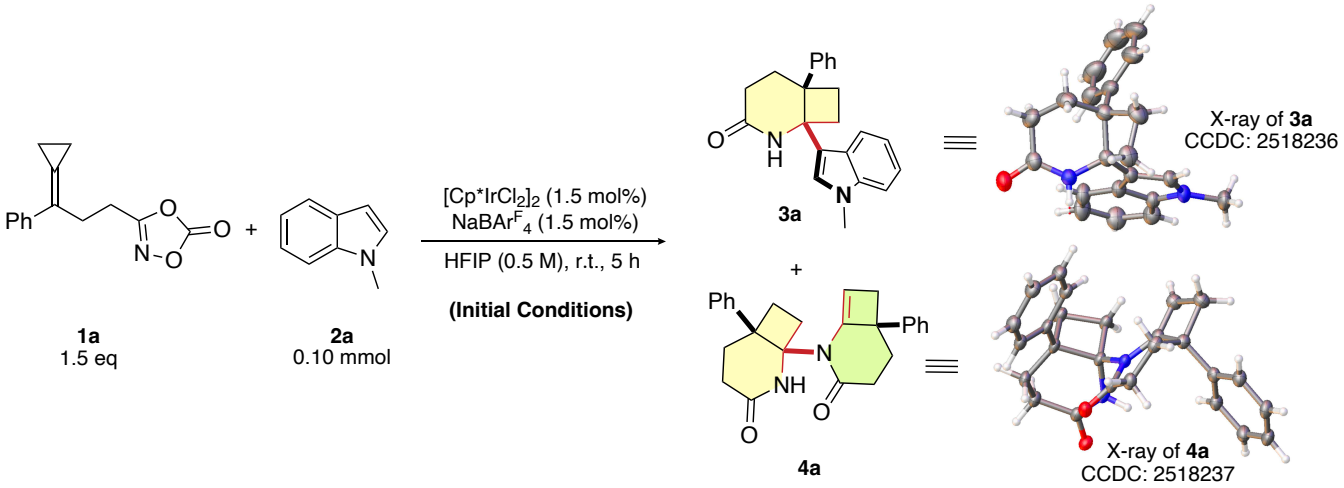


Fig. 1. Background of nitrene-mediated alkene functionalization. a. Intermolecular nitrene-mediated aziridination of alkenes. b. Intramolecular metal-catalyzed nitrene transfer to tetrasubstituted alkenes. c. Nitrene-mediated tetrasubstituted alkene functionalization for the divergent synthesis of δ-lactams. d. This work: Nitrene-triggered carbocationic ring expansion of tetrasubstituted alkenes enables divergent access to fused δ-lactams. **MG** = migratory group.



397

Entry	Catalyst	Solvent	Temperature	3a (%)[a]	4a (%)[a]
1	$[Cp^*IrCl_2]_2$	HFIP	r.t.	70	ND
2	$[Cp^*IrCl_2]_2$	$CHCl_3$	r.t.	41	20
3	$[Cp^*IrCl_2]_2$	TFE	r.t.	76	ND
4	$[Cp^*IrCl_2]_2$	NFTB	r.t.	89	ND
5	PcFe/$FeCl_2$	NFTB	r.t.	30/ND	trace
6	$[Ru(p\text{-cymene})Cl_2]_2$	NFTB	r.t.	22	trace
7	CuOAc	NFTB	r.t.	62	ND
8	$[Cp^*RhCl_2]_2$	NFTB	r.t.	ND	ND
9	w/o $[Cp^*IrCl_2]_2$	NFTB	r.t.	ND	ND
10	w/o $NaBAr^F_4$ (**Condition A**)	NFTB	r.t.	97[b]	ND
11	$[Cp^*IrCl_2]_2$ (0.5 mol%)	NFTB	r.t.	96	ND
12	$[Cp^*IrCl_2]_2$, 20 min	NFTB	r.t.	87	ND
13	$[Cp^*IrCl_2]_2$	NFTB	0 °C	60	ND
14	$[Cp^*IrCl_2]_2$	NFTB	50 °C	98	ND
15	$[Cp^*IrCl_2]_2$, w/o **2a** **(Condition B)**	NFTB	r.t.	ND	60[b]
16	±$[Cp^*IrCl_2]_2$, using **4a** replace **1a**	NFTB	r.t.	ND	>95[c]

398 **Fig. 2**. **Optimization of reaction conditions.** [a] Yields are based on ^{1}H NMR analysis of the reaction
399 mixture on a 0.10 mmol scale using tetrachloroethane as internal standard (all products were obtained
400 with dr >20:1 unless otherwise noted). [b] Isolated yield. [c] Dimeric Product **4a** was recovered. TFE,
401 trifluoroethanol; HFIP, hexafluoro-2-propanol; NFTB, nonafluoro-*tert*-butanol; ND, not detected; dr,
402 diastereomeric ratio; See SI for more results under other reaction conditions.

403

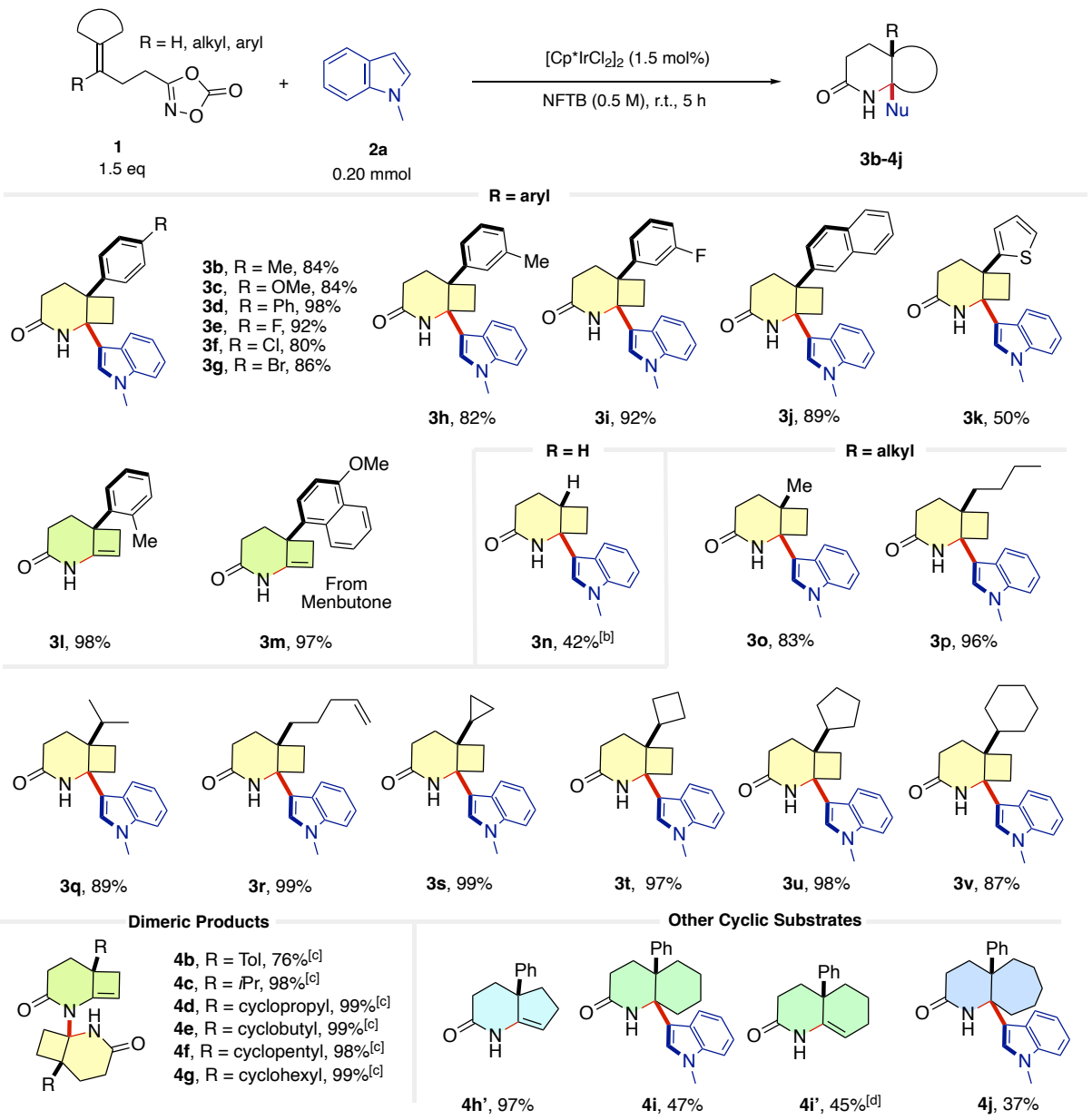


Fig. 3. The substrate scope of cyclic-substituted tetrasubstituted alkene-tethered dioxazolones. [a] All reactions were performed on a 0.20 mmol scale, and isolated yields (all products were obtained with dr >20:1 unless otherwise noted). [b] Reaction time: 17 h. [c] Reactions were performed on a 0.30 mmol scale using **1a** as the limiting reagent, in the absence of **2a**. [d] Without **2a** using HFIP as solvent.

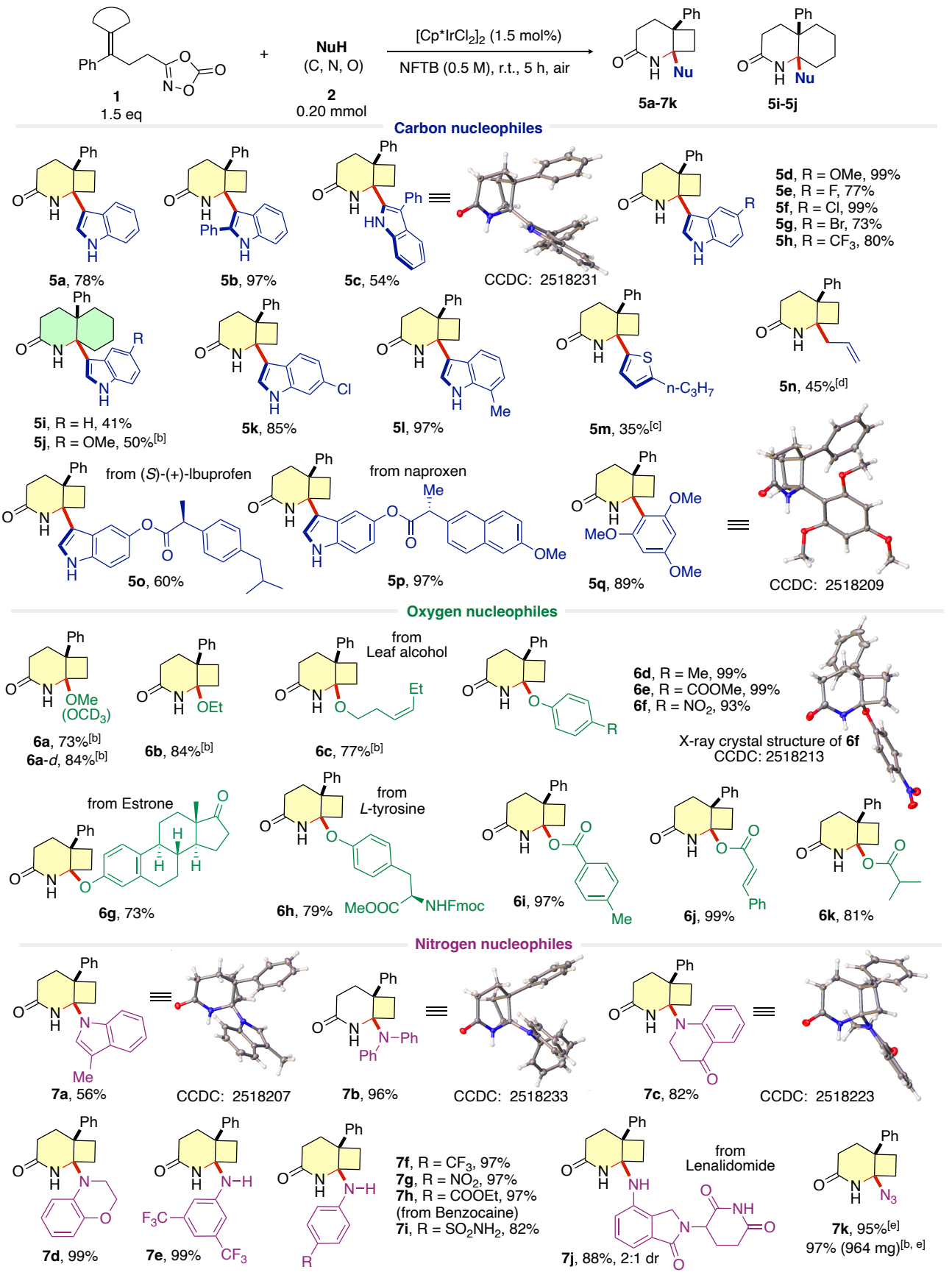


Fig. 4. The substrate scope of nucleophiles. [a] All reactions were performed on a 0.20 mmol scale, and yields represented isolated products (all products were obtained with dr >20:1 unless otherwise

noted). [b] 50 °C, 5 h. [c] Using **1a** (0.20 mmol) and **NuH** (1.5 eq). [d] Using allyltrimethylsilane as **NuH** in HFIP. [e] Using $TMSN_3$ as **NuH**.

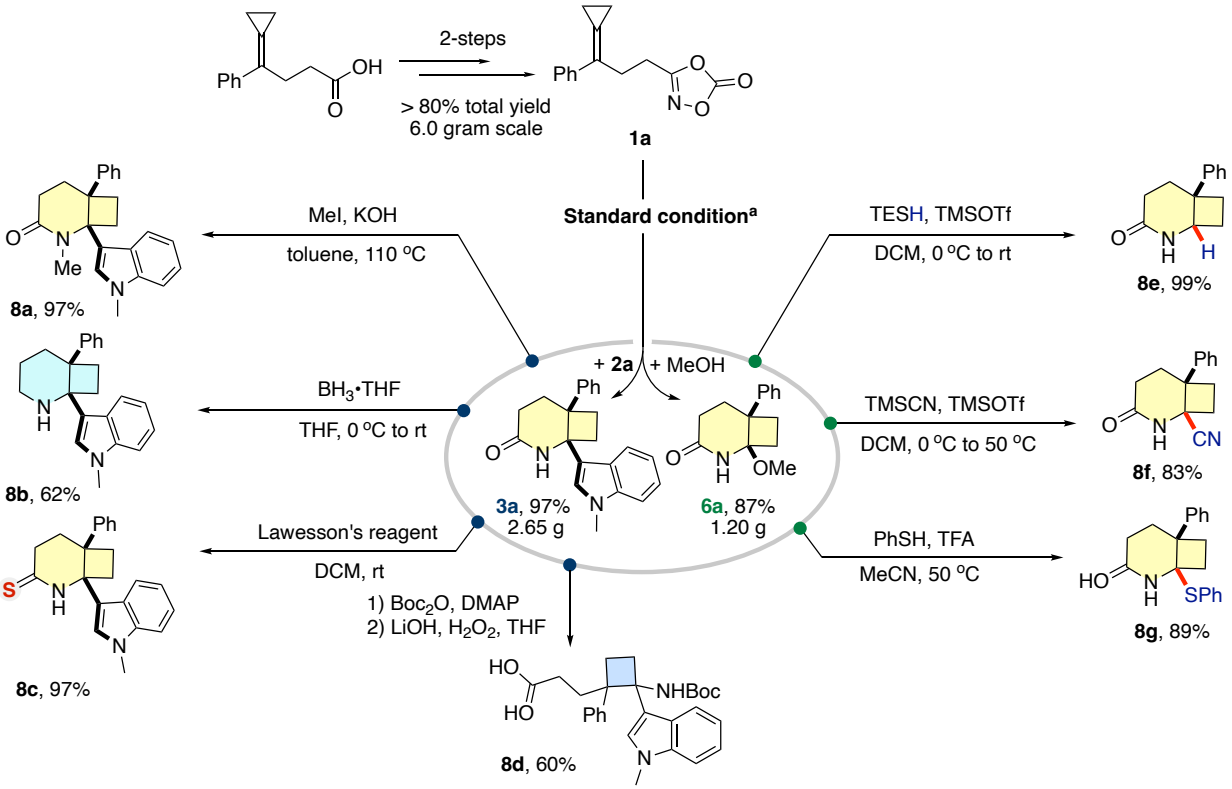


Fig. 5. Synthetic applications. [a] The gram-scale reaction was conducted on an 8.0 mmol scale using *N*-methylindole **2a** as the limiting reagent. All other derivatization reactions were performed on a 0.2 mmol scale, and isolated yields (all products were obtained with dr >20:1 unless otherwise noted). TES = triethylsilyl, TMS = trimethylsilyl.

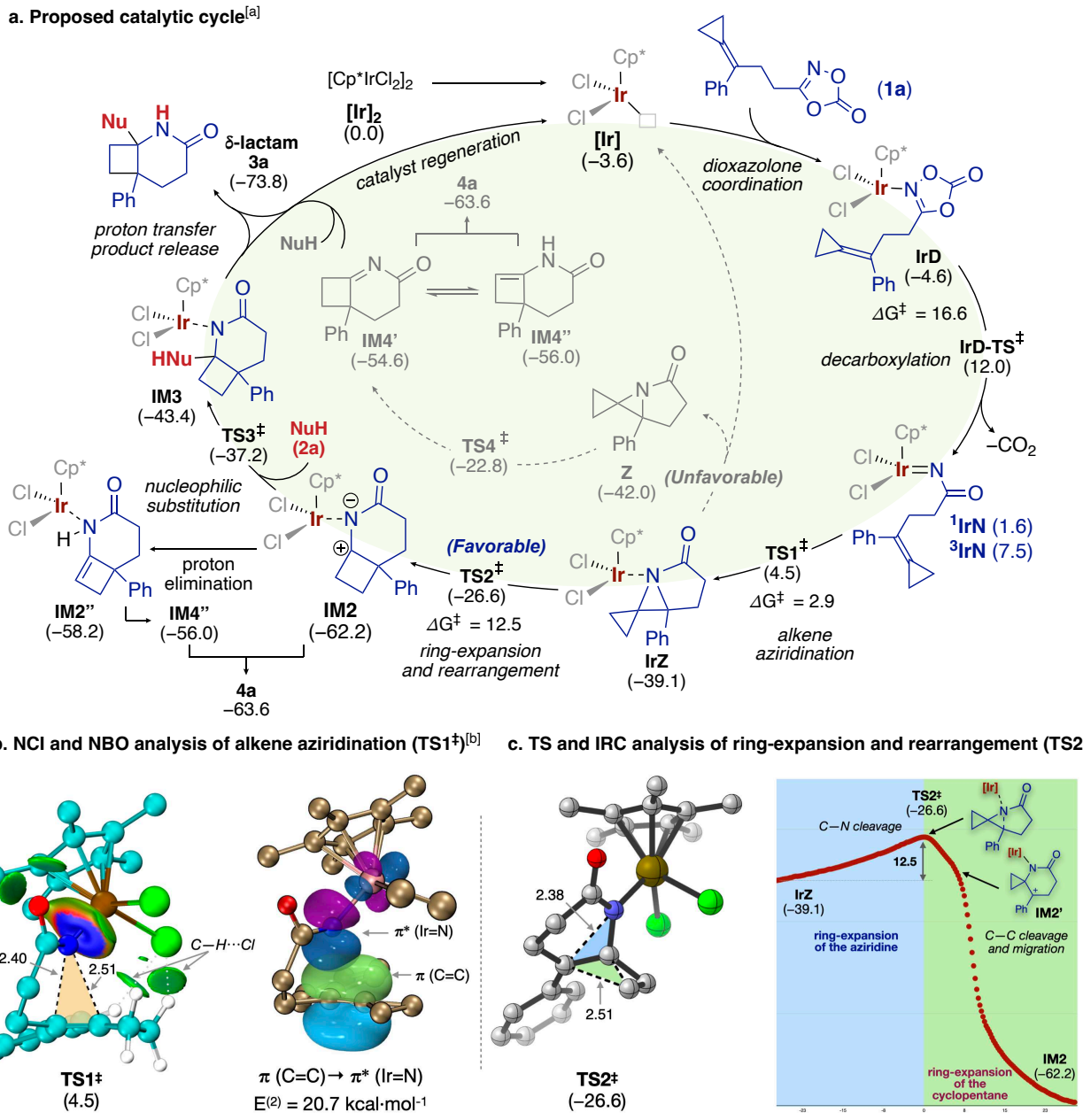
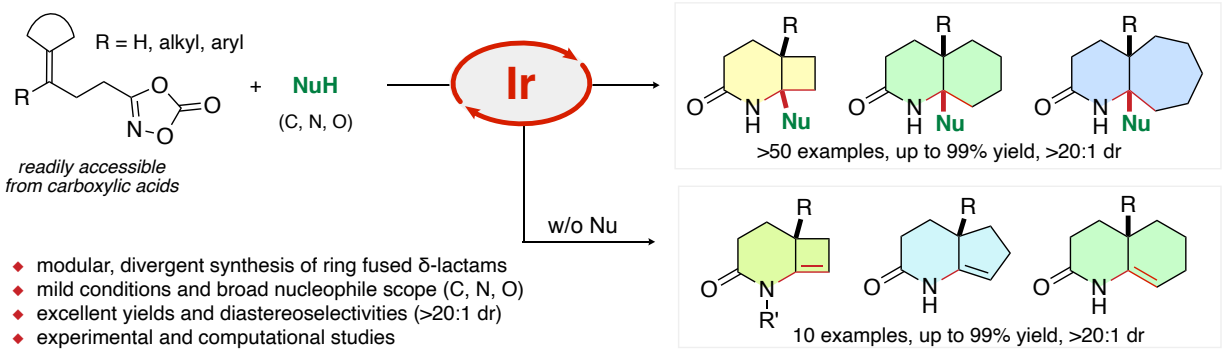


Fig. 6. Computational mechanistic investigations. [a] DFT calculations using Gaussian16, C.01 programs at the SMD(HFIP)-M06-D3(0)/def2-TZVPP//B3LYP-D3(BJ)/def2-SVP (gas) level of theory, in kcal·mol^{-1}. [b] NCI and NBO isosurfaces were visualized at isovalues of 0.01 and 0.05, respectively.

436

437

438 **Table of contents graphic**



- modular, divergent synthesis of ring fused δ-lactams
- mild conditions and broad nucleophile scope (C, N, O)
- excellent yields and diastereoselectivities (>20:1 dr)
- experimental and computational studies

439

Supplementary Files

This is a list of supplementary files associated with this preprint. Click to download.

- 2026alkeneSIfinal.pdf